Bioelectrochemistry 165 (2025) 108994

Contents lists available at ScienceDirect

Bioelectrochemistry

journal homepage: www.journals.elsevier.com/bioelectrochemistry

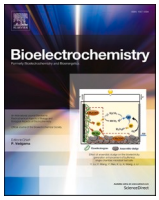

Effective targeting of E2F1 transcription factor via siRNA gene electrotransfer in HT-29 colorectal carcinoma xenografts

Tanja Jesenko [a,b,1], Simona Kranjc Brezar [a,b,1], Ziva Pisljar [a], Tim Bozic [a], Bostjan Markelc [a,c], Monica Cazzato [d], Gabriele Grassi [e,**], Maja Cemazar [a,f,*]

[a] Institute of Oncology Ljubljana, Zaloska cesta 2, Ljubljana 1000, Slovenia
[b] Faculty of Medicine, University of Ljubljana, Vrazov trg 2, Ljubljana 1000, Slovenia
[c] Biotechnical faculty, University of Ljubljana, Jamnikarjeva ulica 101, Ljubljana 1000, Slovenia
[d] University of Trieste, Piazzale Europa 1, Trieste 34127, Italy
[e] Clinical Department of Medical, Surgical and Health Sciences, Cattinara University Hospital, Trieste University, Strada di Fiume 447, I-34149 Trieste, Italy
[f] Faculty of Health Sciences, University of Primorska, Polje 42, Izola 6310, Slovenia

ARTICLE INFO

Keywords:
E2F1
Silencing
siRNA
Colorectal carcinoma
Gene electrotransfer
GET

ABSTRACT

Colorectal cancer (CRC) remains a significant global health concern, with survival outcomes heavily dependent on the stage at diagnosis. Targeted therapies offer a promising approach to improve patient outcomes, particularly by addressing molecular drivers of tumor progression. One such target is the E2F1 transcription factor, a key regulator of the cell cycle and a contributor to proliferation, differentiation, apoptosis, metastasis, and chemoresistance in CRC. Previous studies have demonstrated the efficacy of E2F1 silencing via siRNA-loaded nanoliposomes in reducing tumor cell growth, but challenges such as immunogenicity and off-target effects have limited their in vivo application. In this study, we evaluated the potential of gene electrotransfer (GET) as a non-viral delivery system for delivery of therapeutic siRNA targeting E2F1 in the HT-29 CRC model. In vitro experiments showed effective silencing of E2F1 expression and a significant reduction in HT-29 cell survival. Subsequent in vivo studies confirmed the therapeutic potential of siE2F1 GET, with results demonstrating tumor growth delay, decreased proliferation, and increased necrosis in the tumors. This study establishes proof-of-principle for targeting E2F1 in CRC using GET, showcasing its versatility and therapeutic potential.

1. Introduction

Colorectal cancer (CRC) remains one of the most prevalent cancers globally [1]. While incidence rates have been declining in high-income countries due to widespread implementation of effective screening programs, CRC still poses a growing concern. Prognosis strongly depends on the stage at diagnosis, with early-stage cancers exhibiting significantly higher survival rates compared to advanced stages. Treatment strategies primarily involve surgical resection for cases amenable to surgery. For non-resectable or metastatic CRC, standard therapies include chemotherapy, radiotherapy, immunotherapy, and targeted therapies. However, these treatments face significant limitations. Chemotherapy and radiotherapy often lack specificity, leading to cytotoxic effects on normal cells and resulting in adverse side effects and secondary complications. Targeted therapies and immunotherapies, while offering more precise mechanisms of action, frequently encounter resistance mechanisms within cancer cells, diminishing their clinical efficacy [2]. This underscores the urgent need for novel therapeutic strategies that can enhance specificity, minimize toxicity, overcome resistance, and improve the survival of patients in CRC management [3].

One of the possible molecular targets in CRC is the E2F1 transcription factor. Its expression was found to be increased in CRC compared to normal tissue controls [4]. It is one of the crucial proteins involved in cell cycle regulation, particularly in facilitating the G1 to S phase transition by driving the expression of genes necessary for DNA synthesis and cell division [5]. Besides involvement in cell proliferation, E2F1 has

* Corresponding author at: Institute of Oncology Ljubljana, Zaloska 2, 1000 Ljubljana, Slovenia.
** Corresponding author at: Clinical Department of Medical, Surgical and Health Sciences, Cattinara University Hospital, Trieste University, Strada di Fiume 447, I-34149 Trieste, Italy.
E-mail addresses: ggrassi@units.it (G. Grassi), mcemazar@onko-i.si (M. Cemazar).
[1] Authors contributed equally.

https://doi.org/10.1016/j.bioelechem.2025.108994
Received 21 February 2025; Received in revised form 22 April 2025; Accepted 24 April 2025
Available online 25 April 2025

been linked to differentiation, apoptosis, metastasis and chemoresistance of CRC [6,7]. This makes E2F1 a compelling candidate for therapeutic targeting with therapeutics that downregulate its expression or block its action.

One of the options is E2F1 silencing via RNA interference. The siRNA molecules targeting the transcription factor E2F1 were previously successfully encapsulated into nanoliposomes and employed to target HT-29 human CRC cell lines and human intestinal biopsies [8]. These siRNA-loaded nanoliposomes demonstrated significant efficacy in downregulating E2F1 expression in cultured cells, leading to a notable reduction in cell growth [8]. Additionally, the nanoliposomes exhibited remarkable uptake and target silencing efficiencies in cultured human colonic mucosa biopsies [8]. These findings highlight E2F1 as a promising therapeutic target in colon cancer and demonstrate the feasibility of siRNA-based approaches for its silencing. However, while nanoliposomes show high potential for siRNA delivery, their use in vivo is often hindered by limitations such as immunogenicity, poor stability, and off-target effects due to limited targeting specificity [9–11]. These challenges underscore the need to explore alternative non-viral delivery systems, which may offer enhanced performance, particularly in in vivo applications.

Gene electrotransfer (GET) emerges as a promising non-viral delivery of siRNAs, potentially overcoming some of the constraints associated with nanoliposome-based approaches. This method relies on electroporation, a process where applied electric pulses transiently permeabilize cell membranes by inducing a transmembrane voltage that surpasses physiological thresholds [12]. Electroporation is versatile, enabling the delivery of a broad range of molecules, from small drugs to large nucleic acids. When electroporation is used to deliver nucleic acids, it is called GET [13]. GET is suitable for delivery of different nucleic acids, from smaller RNA molecules to larger plasmid DNA molecules. Notably, GET has been successfully employed for the intratumoral delivery of siRNAs in mouse tumor models [14–16]. The underlying mechanism of siRNA entry following electroporation has been elucidated, revealing a direct transfer of the negatively charged siRNA into the cell cytoplasm exclusively on the side facing the cathode and subsequent diffusion in the cytosol [17]. Interestingly, the mechanism of siRNA uptake is distinct from that observed during the electrotransfer of small molecules or plasmid DNA, underscoring the unique physicochemical properties of siRNAs [17].

In clinical practice, electroporation is predominantly employed for the delivery of cytotoxic drugs, a procedure known as electrochemotherapy [18,19]. This technology is utilized in multiple centers worldwide and is primarily applied to treat cutaneous and subcutaneous lesions due to their accessibility [20,21]. However, promising results have also been reported in the treatment of deep-seated tumors during open surgery or percutaneously, predominately in liver tumors, either primary hepatocellular carcinoma or metastases of CRC [20,22–27]. Additionally, it has also showed potential in treatment of CRC using endoscopic or laparoscopic electrodes [27,28]. As the technology continues to evolve, the use of electroporation is increasingly recognized for its versatility, particularly in the context of GET. Early clinical studies across various tumor types have already demonstrated the safety and feasibility of GET, facilitating broader clinical applications [29–33].

The aim of this study was to evaluate the potential of GET for delivering therapeutic siRNA molecules targeting the E2F1 transcription factor in HT-29 human CRC model. First, in vitro experiments were performed to assess the extent of E2F1 silencing and its cytotoxic effects on HT-29 tumor cells after delivery of siRNAs via lipofection or GET. Subsequently, the approach was tested in vivo using the HT-29 xenograft tumor model to evaluate the transfection efficiency of siRNA delivered via GET, determine the antitumor efficacy of siE2F1 GET, and analyze its effects on proliferation and necrosis in the tumors.

2. Materials and methods

2.1. Cell lines

The HT-29 human CRC cell line was purchased from American Type Culture Collection (HTB-38, ATCC, Manassas, VA, USA). Cells were cultured in Advanced Minimum Essential medium (AMEM, Gibco, Thermo Fisher Scientific, Walthan, MA, USA), supplemented with 5 % (*v*/v) fetal bovine serum (FBS, Gibco), 10.000 units/mL penicillin and 10 mg/mL streptomycin (100 × penicillin–streptomycin, Sigma Aldrich, Darmstadt, Germany) and 1 % (v/v) GlutaMAX (Gibco). Cells were maintained at 37 °C in a 5 % CO_2 humidified atmosphere and they were subcultured twice weekly. HT-29 cells were routinely tested for mycoplasma infection using the MycoAlert™ PLUS Mycoplasma Detection Kit (Lonza, Basel, Switzerland) and were mycoplasma-free.

2.2. Small interfering RNA (siRNA)

The sense sequence of the siRNA targeting E2F1 transcription factor (siE2F1) was 5'-GAGGAGUUCAUCAGCCUUUTT-3′ and of the negative control siRNA targeting luciferase mRNA (siGL2) was 5'-CGUACGCGGAAUACUUCGATT-3′. The sequences were optimized and validated in previous studies [8,34,35]. The siRNAs were obtained as Alexa Fluor 647 (AF647) labeled, HPLC purified annealed siRNA duplexes (Custom Ambion In Vivo siRNA, Thermo Fisher Scientific) and were reconstituted in saline to 20 μM concentration.

2.3. Lipofection

A single-cell suspension was prepared from a monolayer culture maintained for 48 h. Cells were detached using 0.25 % trypsin-EDTA solution (Gibco) and subsequently collected by centrifugation at 400 ×*g* for 5 min. The pelleted cells were resuspended in culture medium, counted using a hemocytometer, and adjusted to a final concentration of 1.2×10^5 cells/mL. 1.2×10^4 of cells were seeded into the wells of 96-well plate. After 24 h, cells were washed in PBS and cell culture media was replaced with the media without FBS and antibiotics. The lipofection procedure was performed using Lipofectamine RNAiMAX transfection reagent (Thermo Fisher Scientific) in OptiMEM Medium (Gibco) following manufacturer's protocol. For each well 5 pmol of siRNA was used for transfection and the volume ratios of siRNA: Lipofectamine RNAiMAX was 1: 2. Three hours after lipofection, the media was replaced with the complete cell medium and cells were cultured at 37 °C in a 5 % CO_2 humidified atmosphere.

2.4. GET in vitro

A 25×10^6 cells/mL cell suspension was prepared in a cold electroporation buffer (EP buffer; 125 mM sucrose, 10 mM K_2HPO_4, 2.5 mM KH_2PO_4, 2 mM $MgCl_2 \times 6\ H_2O$. A volume of 44 μL of the cell suspension was mixed with 11 μL of siRNAs (200 pmol of siE2F1 or siGL2). The 50 μL of the cell-siRNA mixture was pipetted between stainless steel electrodes with 2 mm gap and the electric pulses were delivered by electric pulse generator (Jouan GHT beta, LEROY Biotech, Saint-Orensde-Gameville, France). 8 square-wave electric pulses with 600 V/cm voltage-to-distance ratio, 5 ms pulse duration and frequency of 1 Hz was used based on our previous experience with siRNA delivery and optimization experiment peformed in vivo [14]. Immediately after pulse delivery (<5 s), the mixture was transferred into a 24-well ultra-low attachment plate and 50 μL of FBS was added to the mixture. Five minutes after GET, 1 mL of the cell culture medium was added, and the resulting suspension of the cells was plated for cell viability assay (1.2×10^4 of cells in each well of 96-well plate) in fully supplemented cell culture medium and the rest of the cells were plated in T75 cell culture flasks for RNA isolation and immunofluorescence staining. Cells were cultured at 37 °C in a 5 % CO_2 humidified atmosphere until the next

procedure.

2.5. Cell viability

72 h after lipofection or GET, cell survival was evaluated using Presto Blue viability assay. In each of 96-well plate, 10 μL of PrestoBlue reagent was added and the fluorescence intensity was measured after 1 h of incubation with Cytation 1 multimodal reader (Agilent Technologies, Santa Clara, CA, USA).

2.6. Determination of E2F1 expression using quantitative real-time PCR (qRT-PCR)

Forty-eight hours after lipofection or in vitro GET, cells were detached from the surface of the tissue culture flask using 0.25 % of trypsin-EDTA. The cells were then collected by centrifugation at 400 ×*g* for 5 min. The resulting cell pellet was used as the starting material for RNA isolation. RNA isolation was performed using the peqGOLD Total RNA Kit (VWR) according to the manufacturer's instructions.

For RNA isolation from tumors, the tumors were snap frozen in liquid nitrogen, crushed with a pestle in a mortar and stored at −80 °C until RNA extraction. TRI reagent (VWR) was used for cell lysis. After the lysis, chloroform was added, and the samples were thoroughly mixed. Following 15 min of incubation, the samples were centrifuged, and upper transparent phase was collected and was used for RNA isolation using the peqGOLD Total RNA Kit, starting with the step of binding to the RNA column. The concentration of the isolated RNA and its purity were determined spectrophotometrically using a Cytation 1 Cell Imaging Multi-Mode Reader (Agilent Technologies) by measuring the absorbance at 260 nm (A_{260}) for RNA concentration and by measuring the A_{260}/A_{280} and A_{260}/A_{230} ratios for assessment of RNA purity. Reverse transcription of 1000 ng of total RNA into cDNA was performed in 20 μL of reaction volume containing template RNA and the SuperScript VILO cDNA Synthesis Kit (Thermo Fisher Scientific), using the C1000 Touch Thermal Cycler (Bio-Rad Laboratories Hercules, CA, USA) according to the manufacturer's instructions. The cDNA was diluted to 2 ng/μL in nuclease free water and stored at −20 °C until subsequent analysis. For each 20 μL PCR reaction, 5 μL of cDNA was mixed with 10 μL of PowerUp™ SYBR™ Green Master Mix, 4.6 μL of DEPC-treated water and 0.4 μL of 10 μM primer mixes for E2F1 transcription factor and housekeeping gene (GUSB: β-glucuronidase). The primer sequences were: hE2F1_F: CCAGGAAAAGGTGTGAAATC, hE2F1_R: AAGCGCTTGGTGGTCAGATT, hGUSB_F: AGGTGATGGAAGAAGTGGTG, hGUSB _R: AGGATTTGGTGTGAGCGATC. The reactions were run on a QuantStudio™ 3 Real-Time PCR System (Thermo Fisher Scientific). The cycling conditions were as follows: 2 min at 50 °C, 2 min at 95 °C, 40 cycles of 15 s at 95 °C and 1 min at 60 °C, and for melting curve determination, 15 s at 95 °C, 1 min at 60 °C, and 15 s at 95 °C. Non-template controls (NTC) were run for each primer set. Data were analyzed using QuantStudio's software (Thermo Fisher Scientific). The Ct values were determined for each primer set and each sample. The analysis was performed by normalizing the expression of E2F1 gene to the housekeeping gene (GUSB) using the ΔCt method.

2.7. Determination of E2F1 expression using immunofluorescence staining

Forty-eight hours after in vitro GET, the cells were detached from the surface of the tissue culture flask using 0.25 % of trypsin-EDTA and collected by centrifugation at 400 ×*g* for 5 min. Cell pellet was resuspended in a cell medium (20 % bovine serum albumin (SERVA, Heidelberg, Germany), 5 % EDTA (Sigma Aldrich) in PBS) in a concentration 2×10^5 cells/mL. Cytological slides were prepared using a cytocentrifuge (Thermo Scientific Shandon Cytospin 4 Cytocentrifuge) by centrifugation of two drops of cell suspension at 700 rpm for 4 min. The slides were immediately fixed in ice-cold methanol absolute. The samples on slides were first circled using a Super HT PAP Pen (Biotium, Fremont, CA, USA) to prevent reagent leakage and washed once for 5 min in PBS. The permeabilization of cells was performed 30 min at room temperature using a permeabilization buffer (5 % donkey serum, 0.5 % Triton X-100, and 22 mg/mL glycine in PBS). The permeabilization was followed with a one hour blocking step in a blocking buffer (2 % donkey serum and 22 mg/mL glycine in PBS) at room temperature. After blocking, slides were incubated overnight at 4 °C in a humidified, light-protected chamber with primary rabbit anti-E2F1 monoclonal antibody (ab288369, Abcam, Cambridge, United Kingdom) diluted 1:200 in blocking buffer. The next day, slides were washed three times with PBS for 5 min and incubated with donkey anti-rabbit Alexa Fluor® 488 secondary antibodies (Jackson ImmunoResearch) diluted 1:500 in PBS for 1 h at room temperature. Slides were washed three times for 5 min in PBS and nuclear counterstaining was performed with Hoechst 33342 (3 μg/mL in PBS, Thermo Fisher Scientific) for 10 min in the dark, followed by three additional 5 min PBS washes. The slides were mounted using ProLong™ Glass Antifade Reagent (Thermo Fisher Scientific) and coverslips were applied and secured with nail polish. Imaging was performed using a LSM 800 confocal microscope (Carl Zeiss, Oberkochen, Germany). The fluorophores Hoechst 33342 and Alexa Fluor 488 were excited with lasers with excitation wavelengths of 405 and 488 nm, respectively. The emitted light was collected sequentially with Gallium Arsenide Phosphide (GaAsP) detector via a variable dichroic and filters at the following wavelengths: 410–545 nm (Hoechst 33342) and 488–545 nm (Alexa Fluor 488). The obtained fluorescence images were visualized and analyzed with Imaris software (Bitplane, Belfast, United Kingdom). Fluorescence intensity was evaluated as the ratio of fluorescence intensity analyzed by "surface" function and the number of cells (nuclei) analyzed by "surface" function. At least 200 cells were analyzed for each experimental group.

2.8. Animals and tumor induction

Female Athymic Nude mice (Hsd:Athymic Nude-Foxn1nu) weighting between 20 and 24 g were used in the experiment. The animals were housed in groups of 4–5 animals in sterile polyacrylamide cages at constant humidity (55 % ± 10 %) and temperature (20–23 °C) with sterile water and sterile food ad libitum and 12 h/12 h light-dark cycle. All animals were allowed an acclimatization period of 14 days. The animals were purchased from Envigo RMS SRL (Udine, Italy). Animal experiments were performed in accordance with the permission of the Administration of the Republic of Slovenia for Food Safety, Veterinary Sector, and Plant Protection (permit number U34401–3/2022/17) and in according to Prepare, Arrive and Observe guidelines [36–38]. Each cage was provided with enrichment (Bio-Serv, Flemington, NJ, USA). Tumors were induced in 14-week-old mice by subcutaneously injecting a suspension of 2×10^6 cells in 100 μL of saline solution (0.9 % NaCl) with a syringe with a 27G needle into the right flank. Tumor growth was followed daily and was measured using a digital caliper (Sylvac SA, Yverdon, Switzerland) starting on day 7 after tumor induction until the tumors reached a volume between 45 and 50 mm^3. The tumor volume was calculated with the following formula: $a \times b \times c \times \pi/6$, where a, b, and c are perpendicular tumor diameters. Once the tumors reached 45–50 mm^3, the mice were randomized into experimental groups.

2.9. GET in vivo

The selection of an appropriate electric pulse protocol is crucial for achieving effective GET. Beyond the pulse parameters, the transfection efficacy is also influenced by the histological characteristics of the tumor that influence the interstitial barriers that DNA face when injected into the tumor [39]. To determine the most suitable pulse protocol for this study, we conducted a preliminary experiment of Cy3 labeled siRNA (Trilencer-27 Fluorescent-labeled transfection control siRNA duplex, Origene, Rockville, MD, USA) delivery into HT-29 tumors (71.5 pmol per tumor). Two commonly employed pulse protocols for GET were

evaluated: high-voltage electroporation pulses typically used in electrochemotherapy (ECT; 8 square wave electric pulses with a voltage-to-distance ratio of 1300 V/cm, a pulse duration of 100 μs, and a frequency 1 Hz) and low-voltage pulses tailored for GET (8 square wave electric pulses with a voltage-to-distance ratio of 600 V/cm, a pulse duration of 5 ms, and a frequency 1 Hz) [40–42].

For delivery of therapeutic siE2F1, mice were randomized into 6 experimental groups of 8 mice for evaluation of antitumor effect and 5 mice for tumor collection and analysis. The six experimental groups consisted of the Control non-treated group (Ctrl), injection of saline and delivery of electric pulses group (EP), injection of therapeutic siRNA group (siE2F1), injection of control siRNA (siGL2), GET of therapeutic siRNA (GET siE2F1) and GET of control siRNA (GET siGL2). The treatment was applied once every day for 3 days. The siRNA was delivered by injection of 40 μL of siRNA solution (800 pmol) in the tumor, followed immediately by delivery of GET electric pulses (8 square wave electric pulses with a voltage-to-distance ratio of 600 V/cm, a pulse duration of 5 ms, and a frequency 1 Hz). During the treatment, mice were under 2 % (*v*/v) of isoflurane anesthesia (Isoflurane; Piramal Healthcare UK Limited, London, UK) delivered via VetFlo inhalation anesthesia (Kent Scientific Corporation, Torrington, CT, USA). The pulses were generated by ELECTRO Cell B10 electric pulse generator (Leroy Biotech, France)/(Betatech, L'Union, France) and delivered using two parallel stainless-steel plate electrodes with a 6 mm distance between them. The 8 pulses delivery occurred in two directions, as after the first 4 pulses the electrodes were turned for 90° to deliver the 4 additional pulses, in order to achieve better coverage of the whole tumor to GET [43]. During GET a conductive gel (FIAB, Vicchio, Italy) was used at the contact of the electrodes and the skin overlaying tumors to ensure good conductivity. The siRNA delivery into the tumors was monitored using the IVIS Lumina XRMS III imaging system (Revvity, Waltham, MA, USA) equipped with a 150 W Tungsten/Halogen lamp for fluorescence excitation. Mice were anesthetized with 2 % (*v*/v) isoflurane and AF647 labeled siRNA fluorescence signal was imaged using Living Image software (Revvity). For excitation a 620/20 nm bandpass filter was used and to collect the emitted light a 670/40 nm bandpass filter was used.

2.10. Evaluation of the antitumor effect

Antitumor effect was evaluated by monitoring tumor growth. The tumor diameters were measured three times per week and recorded in In-Life&Tumor software (Labcat, Innovative Programming Associates, Inc., New Jersey, USA). Tumor volume was calculated with the formula described above and tumor growth curves were constructed to evaluate the progression of the tumors over time. The animals were euthanized when the tumor reached predetermined humane endpoint of a volume of 400 mm^3. The animals were considered cured if they had a complete response and were tumor-free at day 100 after the start of the treatment. Tumor growth delay was determined as the difference in the doubling time of tumors between the control group and the treated group. Animal weight loss was monitored at every tumor measurement as a sign of systemic toxicity of the treatments.

2.11. Tumor collection

Tumors were collected 24 h after the last (third) therapy. Three hours prior to tumor collection, the mice were intraperitoneally injected with 200 μL of 10 mg/mL EdU solution (2 mg/mice) (5-ethynyl-2′-deoxyuridine; Abcam, Cambridge, United Kingdom), which marks proliferating cells. After 3 h, the animals were sacrificed, and tumors were excised for immunohistological stainings. The samples were first fixed in 4 % paraformaldehyde (PFA) for 12–16 h at 4 °C. Thereafter, tumors were submerged in 30 % sucrose solution (cryoprotectant) for 24 h at 4 °C, embedded in optimal cutting temperature compound (Tissue-Tek O.C.T. compound, Sakura Finetek, VWR), slowly frozen on dry ice, and stored at −80 °C until processing.

2.12. Histology and immunofluorescence staining

SuperFrost Plus slides (Epredia, Netherlands) with 14-μm-thick tumor sections were prepared from frozen O.C.T. samples using a CM1850 cryostat (Leica, Weltzar, Germay). In the electric pulses' optimization experiment, the slides were used for quantification of transfection efficiency with the detection of the Cy3 labeled siRNA fluorescent signal. Briefly, the slides were washed with 1× PBS for 5 min. Nuclei were stained with 3 μg/mL Hoechst 33342 in PBS for 10 min in the dark. After washing three times for 5 min with PBS, the slides were mounted using ProLong™ Glass Antifade Mountant (Thermo Fisher Scientific), which was left to dry for 48 h in the dark at room temperature (RT) before sealing the edges of the cover glass with nail polish. In the proof-of-principle experiment for siE2F1 delivery, the first slide from each tumor was stained with hematoxylin and eosin (HE) for evaluation of necrosis. The extent of necrosis was evaluated by visual assessment of tumor sections as percentage of tumor necrosis by two independent researchers, blinded to the study. The second slide was used to stain proliferating EdU positive cells and AF647 siRNA signal. Staining was performed in a light-protected, humidified chamber. Before staining, sections were air-dried for 10 min at 37 °C, circled with Mini Super HT PAP Pen, and washed with 1× PBS for 5 min. Afterwards, slides were blocked and permeabilized in block/perm buffer 1 (5 % donkey serum with 0.5 % Triton-X100 and 22.5 mg/mL glycine in PBS) for 1 h at RT in a humidified chamber, and thereafter washed twice in blocking buffer 2 (2 % donkey serum and 22.5 mg/mL glycine in PBS). To detect the incorporated EdU, the Click-iT™ EdU Cell Proliferation Kit for Imaging, Alexa Fluor™ 488 dye (Thermo Fisher Scientific) was used following the manufacturer's instructions. Briefly, slides were incubated with Click-iT mix for 30 min at RT in a humidified chamber and then washed once with blocking buffer 2. After three washes for 10 min each with 1× PBS, nuclei were stained with 3 μg/mL Hoechst 33342 in PBS for 10 min in the dark. After washing three times for 5 min with PBS, the slides were mounted using ProLong™ Glass Antifade Mountant, which was left to dry for 48 h in the dark at RT before sealing the edges of the cover glass with nail polish. Immunofluorescently stained tumor sections were imaged using a Zeiss Axio Observer fluorescence microscope (Carl Zeiss, Oberkochen, Germay) equipped with Colibri 7 LED Light source (UV (385 nm), Violet (430 nm), Blue (475 nm), Green (555 nm), Yellow (590 nm), Red (630 nm), Far Red (735 nm)) and a Hamamatsu Orca Flash 4.0 V3 camera. Emitted light was imaged through the following filters: Filter Set HE BFP shift free (Carl Zeiss) for Hoechst 33342 (nuclei), filter set 38 HE eGFP shift free (Carl Zeiss) for Alexa Fluor 488 (EdU), filter set 112 HE LED (Carl Zeiss) for AF647 (siRNA). The obtained images were visualized and analyzed with Imaris software (Bitplane, Belfast, United Kingdom). The surface of the tumor area was determined based on Hoechst 33342 signal. The surface of the tumor area was determined based on Hoechst 33342 signal. The signal of AF 647 labeled siRNA and Alexa Fluor 488 (EdU) was subsequently masked based on the tumor area (Hoechst 33342 signal), ensuring that analysis was restricted to the relevant regions. To quantify the proliferating cells, the number of Alexa Fluor 488 (EdU) positive nuclei (Hoechst 33342) was determined using the Imaris "Spots" function. Additionally, the surface of the AF647 labeled siRNA signal was determined to quantify the siRNA positive area.

2.13. Statistical analysis

Statistical analysis and graph plotting were performed using GraphPad Prism 9 (La Jolla, CA, USA). Statistical significance was evaluated using one-way ANOVA. A p value <0.05 was considered statistically significant ($^* p < 0.05$). The number of biological replicates (n) are indicated in figure legends.

3. Results

3.1. E2F1 silencing was cytotoxic in HT-29 cells following delivery of siE2F1 via lipofection or GET

The expression of E2F1 molecular target was confirmed by qRT-PCR in HT-29 cell line and HT-29 tumors (Fig. 1A). The expression of E2F1 in the mouse xenografts was comparable to the expression in the cell line and was in the range approximately one fifth of the housekeeping gene GUSB (Fig. 1A). Lipofection of HT-29 cells with siE2F1 efficiency reduced the expression of E2F1 for approximately 50 % (Fig. 1B). The reduction of E2F1 expression via lipofection was accompanied by the reduction of cell survival for approximately 20 % (Fig. 1C). A similar but more potent trend was observed when siE2F1 was delivered via GET. In particular, the expression of E2F1 mRNA was reduced almost for 80 % (Fig. 1D). The cell survival was decreased for approximately 80 % compared to Ctrl cells (Fig. 1E). However, the survival of cells was also reduced for 60 % following electroporation only or delivery of control siRNA siGL2 via GET (Fig. 1E). The silencing of E2F1 protein expression was confirmed by immunofluorescence staining with approximately 40 % reduction of fluorescence intensity following GET siE2F1 (Fig. 1F and G).

3.2. Delivery of siE2F1 via GET induced antitumor effect in HT-29 tumors

In the preliminary experiment, the optimization of the electric pulse parameters was performed. The results demonstrated a clear advantage of the low-voltage GET protocol in terms of transfection efficiency. Following a single GET of Cy3 labeled siRNA, the low-voltage pulses achieved a transfection efficacy of around 30 % of tumor area, compared

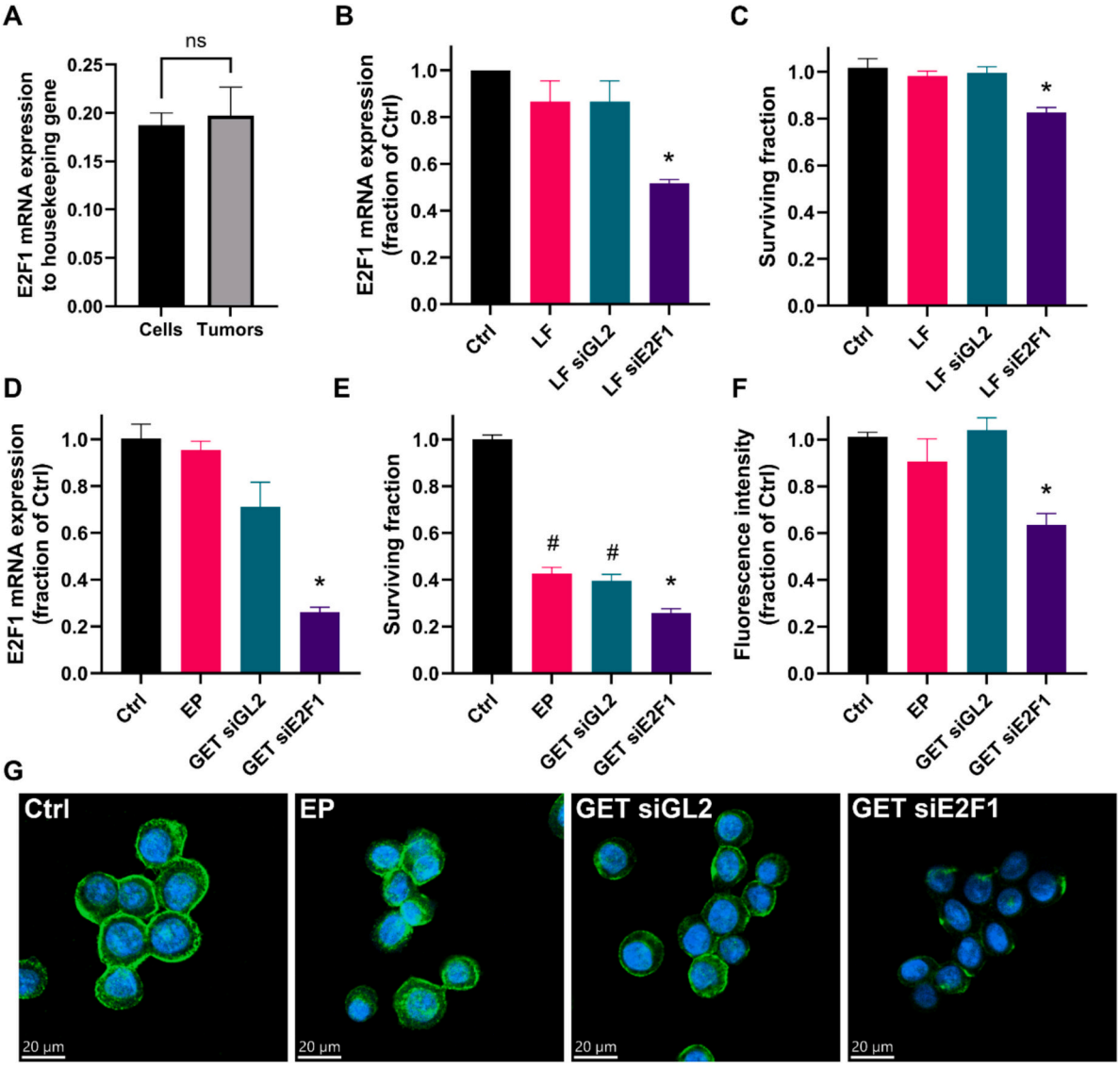

Fig. 1. Reduced expression of E2F1 transcription factor and survival of HT-29 cells after delivery of siE2F1 via lipofection (LF) or GET. (A) Expression of E2F1 mRNA in HT-29 cells and tumors normalized to the GUSB housekeeping gene, $n = 5$. (B) Expression of E2F1 in HT-29 cells after lipofection with therapeutic siE2F1 or control siGL2 siRNA, $n = 3$. (C) HT-29 cell survival after lipofection with therapeutic siE2F1 or control siGL2 siRNA, n = 3. (D) Expression of E2F1 in HT-29 cells after GET of therapeutic siE2F1 or control siGL2 siRNA, n = 3. (E) HT-29 cell survival after GET of therapeutic siE2F1 or control siGL2 siRNA, n = 3. (F) Fluorescence intensity demonstrating E2F1 protein expression after GET of therapeutic siE2F1 or control siGL2 siRNA, $n = 4$. (G) Representative immunofluorescence images of HT-29 stained for E2F1 (green) and nuclei (blue), scale bar = 20 μm. Ctrl, control cells; LF, lipofection with empty lipid particles; LF siE2F1, lipofection with therapeutic siRNA siE2F1; LF siGL2, lipofection with control siRNA siGL2; EP, delivery of electric pulses; GET siE2F1, GET of therapeutic siRNA siE2F1; GET siGL2, GET of control siRNA siGL2. Presented is the arithmetic mean and standard error of the mean. * $p < 0.05$ vs Ctrl, LF, LF siGL2 or Ctrl, EP, GET siGL2; # $p < 0.05$ vs Ctrl. (For interpretation of the references to color in this figure legend, the reader is referred to the web version of this article.)

to only 8 % observed with the high-voltage ECT pulses (Fig. 2). Based on these findings, the low-voltage pulse protocol was selected for GET of therapeutic siE2F1 in the current study.

The siRNA molecules were delivered via GET into HT-29 tumors once a day for three consecutive days. The siE2F1 molecules were effectively delivered into the tumors as demonstrated by imaging of tumors 24 h after the first GET. The GET siE2F1 group demonstrated higher fluorescence intensity in the tumors (denoted as GET) compared to injection of siE2F1 only (denoted as Injection) (Fig. 3A). There was no fluorescence signal detected in the control group (denoted as Ctrl) (Fig. 3A). 24 h after the third GET, delivery of siRNAs was also evaluated in the tumor sections by determining the area of siRNA fluorescent signal (red) normalized to the area of whole tumor sections (blue) (Fig. 3B). Approximately 20 % of tumor area was positive for siRNA signal in the groups of GET (GET siE2F1 and GET siGL2), confirming that both siRNAs were delivered into the tumors to similar extent (Fig. 3C). Some background positive signal was also observed in the EP group due to auto fluorescence of necrotic areas (Fig. 3B).

The antitumor effect of siRNA delivery was evaluated by following the tumor growth and calculation of the tumor growth delay. The treatment of tumors with GET siE2F1 demonstrated high antitumor efficacy. The delivery of siE2F1 via GET significantly delayed the growth of tumors (up to 20 days) compared to all other control groups (Ctrl, EP, siE2F1, siGL2, GET siGL2) (Fig. 3D and E). One mouse from the GET siE2F1 had a complete response and was tumor-free for 100 days after the therapy and was therefore termed cured. There were no complete responses in other groups. Treatment of tumors with control siGL2 GET (GET siGL2) or electric pulses only (EP) also induced some tumor growth delay (up to 5.6 days) (Fig. 3D and E).

3.3. Delivery of siE2F1 via GET induced necrosis and reduced proliferation in HT-29 tumors

The antitumor effect was further evaluated by determination of necrosis and proliferation in the tumors. The delivery of siE2F1 via GET significantly increased the amount of necrosis in the tumor areas 24 h after the last therapy (Fig. 4A). The extent of necrosis in the siE2F1 tumors was high, around 80 %, which sometimes resulted in necrosis of the tumor center (Fig. 4A, GET siE2F1). The extent of necrosis was also significantly increased in GET siGL2 group (Fig. 4A) compared to Ctrl but to a lesser extent as in therapeutic GET siE2F1 group (Fig. 4A). There was some minor extent of necrosis observed in the EP group, which was not significant (Fig. 4A). GET of both siRNAs, therapeutic siE2F1 and control siGL2, significantly reduced the proliferation in the tumors as indicated by decreased number of EdU positive cells in the tumor sections (Fig. 4B). Both treatments decreased proliferation to similar extent.

4. Discussion

This study demonstrates the successful application of GET to deliver siRNA targeting E2F1, achieving effective silencing of E2F1 expression and a significant reduction in the survival of HT-29 CRC cells. The in vivo delivery of siE2F1 further confirmed its therapeutic potential, as evidenced by a pronounced antitumor effect, including delayed tumor growth, reduced proliferation in the tumors, and increased tumor necrosis. These findings establish a proof-of-principle for targeting E2F1 in CRC, highlighting its potential as a viable therapeutic target and laying the groundwork for future studies to refine and optimize this approach.

Oligonucleotides have emerged as a promising class of therapeutics in cancer treatment due to their ability to modulate gene expression with high specificity [44]. These short, synthetic strands of nucleotides can be designed to target oncogenes, tumor suppressor genes, or other molecular pathways critical for cancer progression [45]. Among the most common types are siRNA molecules. The selection of siRNA sequences is critical to ensuring the efficiency and specificity of gene silencing in tumor-targeted therapies [46]. An optimal siRNA sequence must effectively target the mRNA of the gene of interest to induce robust and sustained knockdown while minimizing off-target effects that could compromise the safety and efficacy of the treatment. In our study, we employed optimized and validated siRNA sequences specifically designed to target the human E2F1 transcription factor, building on findings from previous studies in multiple cellular models, including colorectal carcinoma, hepatocellular carcinoma and coronary smooth muscle cells [8,34,35,47]. Consistent with these findings, our results demonstrated approximately 80 % silencing at the mRNA level and approximately 40 % at the protein level after GET siE2F1. These data collectively confirm the robustness and specificity of the siE2F1 sequence, supporting its effective design and performance.

E2F1 plays a multifaceted role in CRC, driving cell proliferation, apoptosis and drug resistance [6]. These functions make E2F1 an appealing molecular target for the development of novel cancer therapies. However, targeting E2F1 requires careful consideration, as it is also essential for normal cellular processes such as transcription regulation, DNA-damage repair and metabolism [5,48,49]. Systemic pan-inhibition of E2F1 could therefore lead to significant off-target effects and toxicity. This limits the use of lipid particles (lipofection) as a systemic administration in vivo. To address these challenges, localized delivery methods, such as GET, offer a promising solution. Our results

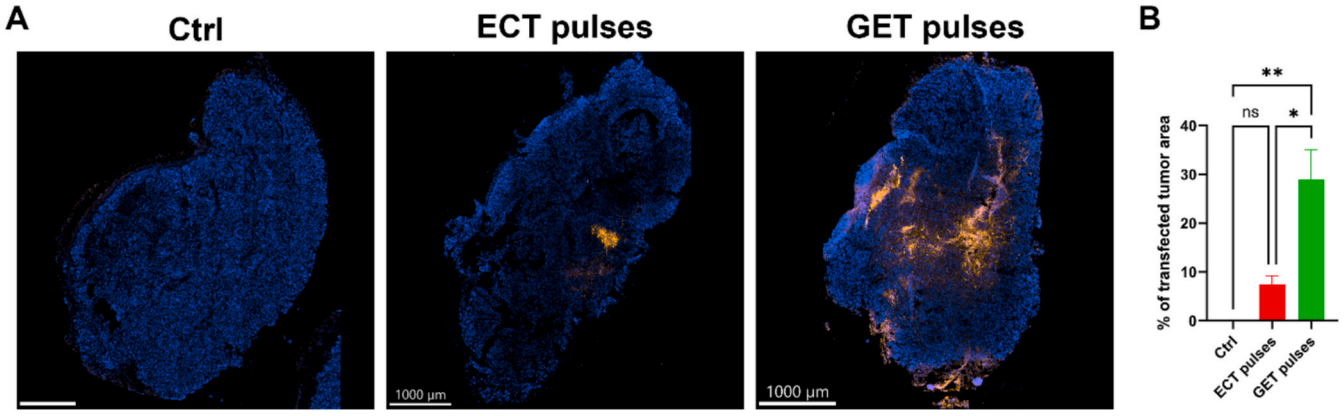

Fig. 2. Transfection efficiency of two pulse protocols for delivery of Cy3 labeled siRNA. (A) Representative images of transfected tumors. Orange color represent siRNA and blue color the tumor stained with nuclear stain Hoechst 33342. Scale bar = 1000 µm. Ctrl – untreated tumor; ECT pulses - 8 pulses, 1300 V/cm, 100 µs, 1 Hz; GET pulses: 8 pulses, 600 V/cm, 5 ms, 1 Hz. (B) Percent of transfected tumor area calculated as the area of Cy3 signal divided with the area of tumor (Hoechst). Presented is the arithmetic mean and standard error of the mean. $n = 3$; * $p < 0.05$ ECT pulses vs GET pulses, ** $p < 0.05$ Ctrl vs GET pulses. (For interpretation of the references to color in this figure legend, the reader is referred to the web version of this article.)

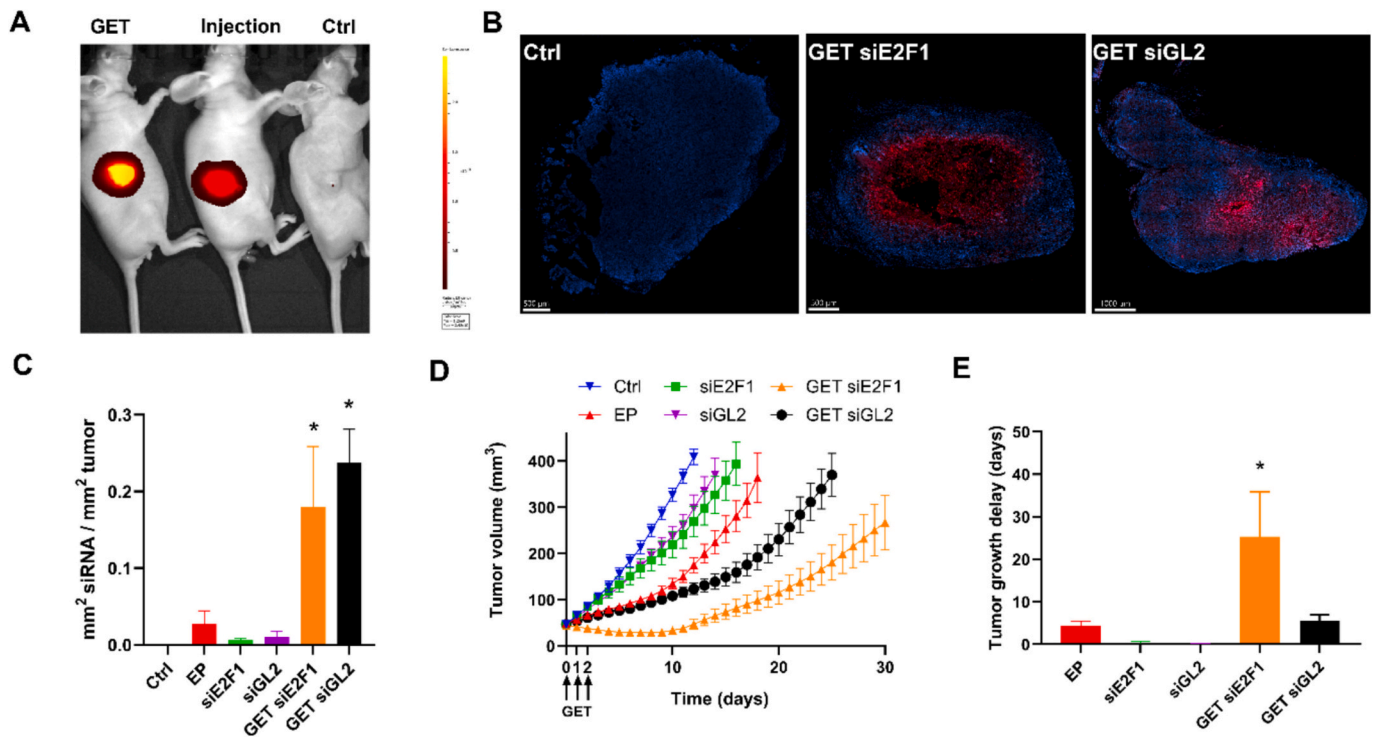

Fig. 3. Delivery of siRNAs and antitumor effect of siE2F1 in HT-29 tumors. (A) Fluorescent signal of AF647 labeled siRNA in the tumors 24 h after the first treatment. Mouse on the left from GET siE2F1 group demonstrated the highest fluorescence intensity in the tumors (denoted as GET). The mouse in the middle received injection of siE2F1 only (denoted as Injection) and demonstrated lower fluorescence intensity signal in the tumors compared to the left mouse. There was no fluorescence signal detected in the right mouse from the control group (denoted as Ctrl). (B) Images of siRNA fluorescent signal in the tumors 24 h after the last therapy. Red color represents siRNA signal and blue color the nuclei. Scale bar 500 μm for Ctrl and GET siE2F1 and 1000 μm for GET siGL2 image. (C) Evaluation of transfection efficiency 24 h after the last treatment in the tumor sections. The area of siRNA fluorescent signal was evaluated (AF647) and normalized to the tumor area (Hoechst 33342); $n = 5$; * $p < 0.05$ vs Ctrl. (D) Tumor growth curves and (E) tumor growth delay calculated from the tumor curves; $n = 8$; Presented is the arithmetic mean and standard error of the mean. * $p < 0.05$ vs Ctrl, EP, siE2F1, siGL2, GET siGL2. Groups: Control non-treated group (Ctrl), injection of saline and delivery of electric pulses group (EP), injection of therapeutic siRNA group (siE2F1), injection of control siRNA (siGL2), GET of therapeutic siRNA (GET siE2F1) and GET of control siRNA (GET siGL2). (For interpretation of the references to color in this figure legend, the reader is referred to the web version of this article.)

demonstrate that GET achieved superior silencing efficiency of E2F1 (80 %) compared to lipofection (50 %) on the mRNA level, highlighting its effectiveness as a delivery method for siRNA. Beyond enhanced knockdown, GET offers key advantages for translational applications, including targeted, localized delivery to tumor tissue, reduced risk of systemic off-target effects, and a favorable immunological profile compared to lipid-based carriers [9,10,33,50]. These features support the suitability of GET for in vivo use and its potential for clinical translation.

A crucial aspect of gene therapy is the development of an efficient transfection protocol to ensure effective delivery of therapeutic siRNAs. To investigate the effectiveness of different transfection methods for siE2F1 delivery, we compared gene silencing and cell viability outcomes following delivery via lipofection and GET. The delivery of siE2F1 via both transfection methods induced effective silencing of E2F1 expression. GET of siE2F1 induced higher silencing rate in vitro to lipofection indicating on more efficient delivery of siRNA molecules into the cells and confirms the suitability of GET as a delivery system. Using both methods of transfection, the survival of cells was reduced following siE2F1 delivery. Delivery via lipofection reduced cell viability for approximately 20 %, whereas delivery via GET reduced cell viability for almost 80 %. However, the survival of cells treated by electric pulses only (EP) or GET of control siRNA (siGL2) reduced cell survival for around 60 %, which indicates that contribution of siE2F1 silencing on cell survival is of additional 20 %, similarly to lipofection. The 60 % reduction in cell survival can be contributed to non-specific effects of electric pulses, which is frequently observed in the in vitro setting with this pulse protocol [40,41,51].

The non-specific cytotoxicity was also observed in the in vivo setting as both control groups, EP and GET siGL2, induced minor tumor growth delays, induced necrosis and reduced proliferation in the tumors. Although demonstrating some cytotoxic effects, the electric pulses used in this study effectively facilitated siRNA delivery to both cells and tumors, as evidenced by the extent of E2F1 silencing and the monitoring of siRNA uptake through live animal imaging and immunofluorescence analysis. Additional cytotoxic effects were observed in the GET siGL2 group, likely due to the introduction of nucleic acids into the cytosol, which can trigger cell death through the activation of RNA-sensing pathways [52]. However, in our study, these effects were minimized by employing chemically modified in vivo siRNAs to reduce activation of such pathways. However, while the GET siE2F1 exhibited some nonspecific cytotoxic effects, which may contribute to the overall antitumor efficacy of GET siE2F1, the GET siE2F1 treatment demonstrated significantly greater anti-tumor effects compared to the EP or GET siGL2 groups. This highlights the targeted action of E2F1 silencing and its therapeutic potential.

Although electric pulses reduced cell viability and induced a tumor growth delay, this cytotoxic effect may be considered beneficial in the context of cancer therapy. Similar to (electro)chemotherapy or radiotherapy, the ablative effect of GET can contribute to the overall antitumor response, enhancing therapeutic efficacy. Importantly, the surviving cells are efficiently transfected, enabling the specific silencing of target genes such as E2F1. This combined effect of localized cytotoxicity and targeted gene silencing may help overcome resistance mechanisms often observed with targeted therapies [53]. In contrast, for non-cancer applications such as protein replacement therapy or DNA

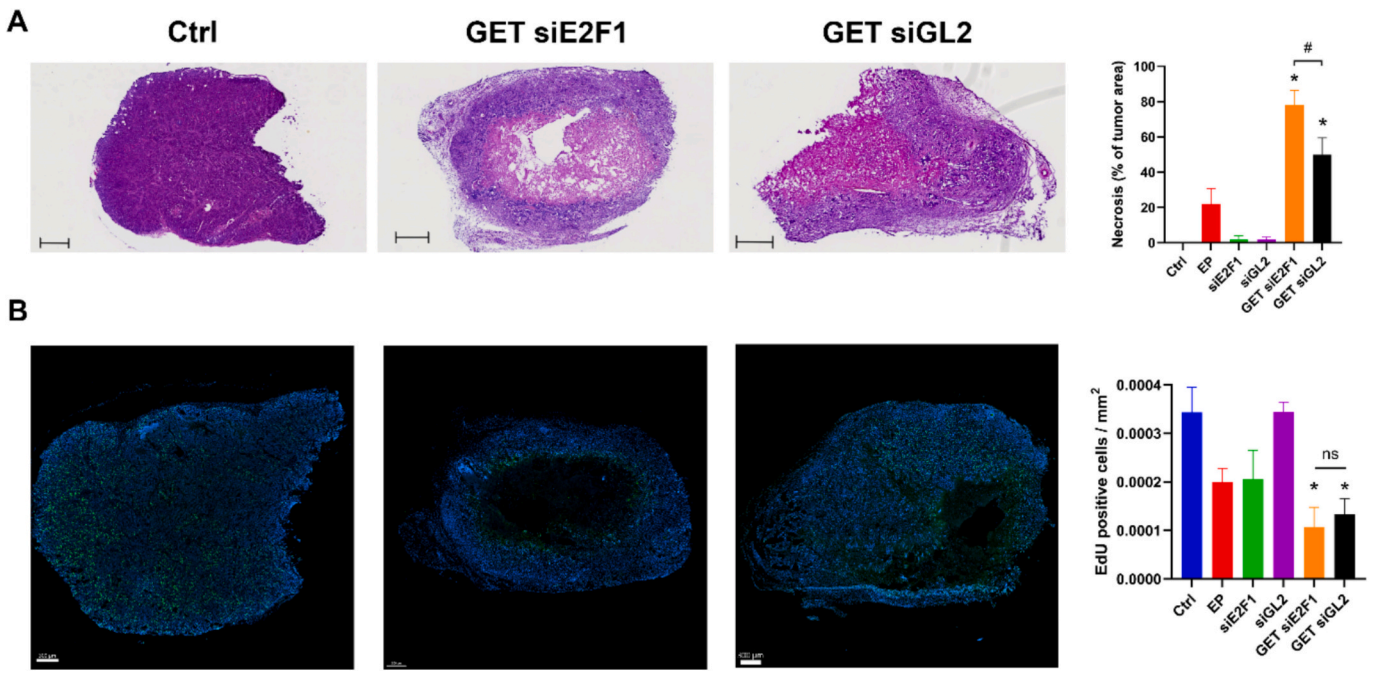

Fig. 4. Increased necrosis and reduced proliferation in the HT-29 tumors after GET siE2F1. (A) HE stained tumor sections and evaluation of percent of necrosis in the tumor sections; scale bar = 500 μm; $n = 5$; * $p < 0.05$ vs Ctrl, EP, siE2F1, siGL2; # $p < 0.05$ GET siE2F1 vs GET siGL2. (B) Immunofluorescent staining of proliferation in tumor sections using EdU labeling (green nuclear staining) and nuclear stain Hoechst 33342 (blue nuclei). The quantification of tumor proliferation as the number of EdU positive cells normalized to the tumor area; scale bar = 300 μm; n = 5; Presented is the arithmetic mean and standard error of the mean. * $p < 0.05$ vs Ctrl. Groups: Control non-treated group (Ctrl), injection of saline and delivery of electric pulses group (EP), injection of therapeutic siRNA group (siE2F1), injection of control siRNA (siGL2), GET of therapeutic siRNA (GET siE2F1) and GET of control siRNA (GET siGL2). (For interpretation of the references to color in this figure legend, the reader is referred to the web version of this article.)

vaccination, minimizing tissue damage is crucial. To address this, noninvasive and low-toxicity GET systems have been developed by our group and others, demonstrating the adaptability of GET parameters to various therapeutic goals [16,54–56].

Electroporation is not selectively toxic to cancer cells and the reduction of normal cell survival was already observed in mouse C2C12 skeletal myoblast cells, Kera-308 keratinocytes and L929 fibroblasts [51,57]. Cell death following the delivery of electric pulses primarily arises from the failure of the cell membrane to reseal after electroporation, leading to irreversible electroporation and a cascade of lethal intracellular events. The disruption of membrane integrity compromises the cell's ability to maintain homeostasis, resulting in uncontrolled ion flux, ATP depletion, and oxidative stress. These perturbations overwhelm cellular repair mechanisms, triggering regulated cell death pathways such as apoptosis, or in cases of severe damage, necrosis. The extent and type of cell death depend significantly on the parameters of the electric pulses, namely their intensity, duration, and number, as well as the cell type and physiological condition [58].

In this study, we employed a previously established GET pulse protocol to ensure efficient delivery of siRNA [14–16]. Although the optimization of pulse parameters such as intensity, duration, and number could potentially reduce cytotoxicity, this was beyond the scope of our proof-of-principle study. In the future, additional dose-response experiments using different pulse settings could help determine the optimal balance between delivery efficiency and the preservation of cell viability.

Our findings of siE2F1 delivery align with our previous studies in hepatocellular carcinoma utilizing a galactosylated polyaspartamide copolymer for delivery of siE2F1 (same siRNA sequence) [47]. In this study, a reduction in E2F1 mRNA expression by approximately 55 % was observed leading to a decrease in cell viability to around 70 % in Huh7 cells. Furthermore, in vivo experiments confirmed the specificity of siE2F1 delivery using the copolymer, leading to a tumor growth delay of up to three days, approximately 20 % reduction of E2F1 mRNA expression and induction of approximately 38 % necrosis in tumors. On one side, the GET approach for delivery of siE2F1 seems to be superior in terms of inducing an antitumor effect compared to delivery via liposomes or galactosylated polyaspartamide copolymer. On the other side, one constraint of the tested GET therapy is that siRNA delivery and silencing are confined to the injection sites, with distribution potentially hindered by interstitial barriers, particularly in dense or compact solid tumor histologies. Consequently, regions of the tumor not reached by the siRNA remain untreated, which can lead to tumor regrowth. In this context, the additional cytotoxic effects of electric pulses are advantageous, as they contribute to tumor cell death beyond siRNA silencing. To enhance the anti-tumor efficacy even further, combined treatment regimens involving local ablative techniques, such as radiotherapy or electrochemotherapy, could be used [59–61]. These approaches could help eradicate residual viable tumor masses that do not undergo GET siE2F1. Furthermore, the study's reliance on a single tumor model represents a limitation, highlighting the need for additional research using diverse tumor xenograft models and immunocompetent mouse models to strengthen the evidence for the therapy's efficacy. Additionally, a detailed investigation into the underlying mechanisms of action is crucial to generate further data that can refine and optimize this therapeutic approach.

CRediT authorship contribution statement

Tanja Jesenko: Writing – original draft, Validation, Investigation, Conceptualization. **Simona Kranjc Brezar:** Writing – review & editing, Visualization, Investigation, Conceptualization. **Ziva Pisljar:** Writing – review & editing, Visualization, Investigation. **Tim Bozic:** Writing – review & editing, Investigation. **Bostjan Markelc:** Writing – review & editing, Methodology. **Monica Cazzato:** Investigation. **Gabriele Grassi:** Writing – review & editing, Resources, Funding acquisition,

Conceptualization. **Maja Cemazar:** Writing – review & editing, Resources, Funding acquisition, Conceptualization.

Declaration of competing interest

The authors declare that they have no known competing financial interests or personal relationships that could have appeared to influence the work reported in this paper.

Acknowledgements

The authors acknowledge the financial support from the Slovenian Research and Innovation Agency (program No. P3-0003). G.G. wish to thank the Italian Ministry of Foreign Affairs and International Cooperation (MAECI), grant number VN21GR01 and the "Lega Italiana per la Lotta Contro I Tumori" (project "Evaluation of a novel antifibrotic and antitumor molecule for hepatocellular carcinoma") for the support.

Data availability

Data will be made available on request.

References

[1] M.S. Hossain, H. Karuniawati, A.A. Jairoun, Z. Urbi, D.J. Ooi, A. John, et al., Colorectal Cancer: a review of carcinogenesis, global epidemiology, current challenges, risk factors, preventive and treatment strategies, Cancers (Basel) 14 (2022) 1732, https://doi.org/10.3390/CANCERS14071732.

[2] H. Fadlallah, J. El Masri, H. Fakhereddine, J. Youssef, C. Chemaly, S. Doughan, et al., Colorectal cancer: recent advances in management and treatment, World J. Clin. Oncol. 15 (2024) 1136–1156, https://doi.org/10.5306/WJCO.V15.I9.1136.

[3] U. Hani, Y.K. Honnavalli, M.Y. Begum, S. Yasmin, R.A.M. Osmani, M.Y. Ansari, Colorectal cancer: a comprehensive review based on the novel drug delivery systems approach and its management, J. Drug Deliv. Sci. Technol. 63 (2021) 102532, https://doi.org/10.1016/J.JDDST.2021.102532.

[4] Z. Xu, H. Qu, Y. Ren, Z. Gong, H.J. Ri, F. Zhang, et al., Systematic analysis of E2F expression and its relation in colorectal Cancer prognosis, Int. J. Gen. Med. 15 (2022) 4849–4870, https://doi.org/10.2147/IJGM.S352141.

[5] M.G. Ertosun, F.Z. Hapil, O.Z.E.S. Osman Nidai, E2F1 transcription factor and its impact on growth factor and cytokine signaling, Cytokine Growth Factor Rev. 31 (2016) 17–25, https://doi.org/10.1016/J.CYTOGFR.2016.02.001.

[6] Z. Fang, M. Lin, C. Li, H. Liu, C. Gong, A comprehensive review of the roles of E2F1 in colon cancer, Am. J. Cancer Res. 10 (2020) 757.

[7] H. Gao, F. Zhou, R. Li, J. Yuan, L. Ye, E2F1 inhibits cellular senescence and promotes oxaliplatin resistance in colorectal cancer, Ann. Transl. Med. 11 (2023) 185, https://doi.org/10.21037/ATM-22-4054.

[8] S. Bochicchio, B. Dapas, I. Russo, C. Ciacci, O. Piazza, S. De Smedt, et al., In vitro and ex vivo delivery of tailored siRNA-nanoliposomes for E2F1 silencing as a potential therapy for colorectal cancer, Int. J. Pharm. 525 (2017) 377–387, https://doi.org/10.1016/J.IJPHARM.2017.02.020.

[9] Y. Lee, M. Jeong, J. Park, H. Jung, H. Lee, Immunogenicity of lipid nanoparticles and its impact on the efficacy of mRNA vaccines and therapeutics, Exp. Mol. Med. 55 (2023) 2085–2096, https://doi.org/10.1038/S12276-023-01086-X.

[10] C.T. Inglut, A.J. Sorrin, T. Kuruppu, S. Vig, J. Cicalo, H. Ahmad, et al., Immunological and toxicological considerations for the Design of Liposomes, Nanomaterials 10 (2020) 190, https://doi.org/10.3390/NANO10020190.

[11] C. Su, Y. Liu, Y. He, J. Gu, Analytical methods for investigating in vivo fate of nanoliposomes: a review, J. Pharm. Anal. 8 (2018) 219–225, https://doi.org/10.1016/J.JPHA.2018.07.002.

[12] T. Kotnik, L. Rems, M. Tarek, D. Miklavcic, Membrane electroporation and Electropermeabilization: mechanisms and models, Annu. Rev. Biophys. 48 (2019) 63–91, https://doi.org/10.1146/ANNUREV-BIOPHYS-052118-115451.

[13] T. Potočnik, A. Maček Lebar, Š. Kos, M. Reberšek, E. Pirc, G. Serša, et al., Effect of experimental electrical and biological parameters on gene transfer by electroporation: a systematic review and Meta-analysis, Pharmaceutics (2022) 14, https://doi.org/10.3390/PHARMACEUTICS14122700.

[14] T. Dolinsek, B. Markelc, G. Sersa, A. Coer, M. Stimac, J. Lavrencak, et al., Multiple delivery of siRNA against endoglin into murine mammary adenocarcinoma prevents angiogenesis and delays tumor growth, PloS One (2013) 8, https://doi.org/10.1371/JOURNAL.PONE.0058723.

[15] A. Paganin-Gioanni, M.P. Rols, J. Teissié, M. Golzio, Cyclin B1 knockdown mediated by clinically approved pulsed electric fields siRNA delivery induces tumor regression in murine melanoma, Int. J. Pharm. (2020) 573, https://doi.org/10.1016/J.IJPHARM.2019.118732.

[16] S.K. Brezar, M. Kranjc, M. Čemažar, S. Buček, G. Serša, D. Miklavčič, Electrotransfer of siRNA to silence enhanced green fluorescent protein in tumor mediated by a high intensity pulsed electromagnetic field, Vaccines (Basel) (2020) 8, https://doi.org/10.3390/VACCINES8010049.

[17] M. Golzio, J. Teissié, Imaging of Electrotransferred siRNA, Methods Mol. Biol. 1372 (2016) 89–97, https://doi.org/10.1007/978-1-4939-3148-4_7.

[18] A.J.P. Clover, F. de Terlizzi, G. Bertino, P. Curatolo, J. Odili, L.G. Campana, et al., Electrochemotherapy in the treatment of cutaneous malignancy: outcomes and subgroup analysis from the cumulative results from the pan-European international network for sharing practice in Electrochemotherapy database for 2482 lesions in 987 patients (2008-2019), Eur. J. Cancer 138 (2020) 30–40, https://doi.org/10.1016/J.EJCA.2020.06.020.

[19] J. Gehl, G. Sersa, L.W. Matthiessen, T. Muir, D. Soden, A. Occhini, et al., Updated standard operating procedures for electrochemotherapy of cutaneous tumours and skin metastases, Acta Oncol. 57 (2018) 874–882, https://doi.org/10.1080/0284186X.2018.1454602.

[20] B. Hadzialjevic, M. Omerzel, B. Trotovsek, M. Cemazar, T. Jesenko, G. Sersa, et al., Electrochemotherapy combined with immunotherapy - a promising potential in the treatment of cancer, Front. Immunol. (2024) 14, https://doi.org/10.3389/FIMMU.2023.1336866.

[21] M. Marty, G. Sersa, J.R. Garbay, J. Gehl, C.G. Collins, M. Snoj, et al., Electrochemotherapy – an easy, highly effective and safe treatment of cutaneous and subcutaneous metastases: results of ESOPE (European standard operating procedures of Electrochemotherapy) study, Eur. J. Cancer Suppl. 4 (2006) 3–13, https://doi.org/10.1016/J.EJCSUP.2006.08.002.

[22] M. Djokic, M. Cemazar, P. Popovic, B. Kos, R. Dezman, M. Bosnjak, et al., Electrochemotherapy as treatment option for hepatocellular carcinoma, a prospective pilot study, Eur. J. Surg. Oncol. 44 (2018) 651–657, https://doi.org/10.1016/J.EJSO.2018.01.090.

[23] M. Djokic, M. Cemazar, M. Bosnjak, R. Dezman, D. Badovinac, D. Miklavcic, et al., A prospective phase II study evaluating intraoperative Electrochemotherapy of hepatocellular carcinoma, Cancers (Basel) 12 (2020) 1–14, https://doi.org/10.3390/CANCERS12123778.

[24] I. Edhemovic, E. Brecelj, M. Cemazar, N. Boc, B. Trotovsek, M. Djokic, et al., Intraoperative electrochemotherapy of colorectal liver metastases: a prospective phase II study, Eur. J. Surg. Oncol. 46 (2020) 1628–1633, https://doi.org/10.1016/J.EJSO.2020.04.037.

[25] M. Djokic, R. Dezman, M. Cemazar, M. Stabuc, M. Petric, L.M. Smid, et al., Percutaneous image guided electrochemotherapy of hepatocellular carcinoma: technological advancement, Radiol. Oncol. 54 (2020) 347–352, https://doi.org/10.2478/RAON-2020-0038.

[26] L. Luerken, M. Doppler, S.M. Brunner, H.J. Schlitt, W. Uller, Stereotactic percutaneous Electrochemotherapy as primary approach for Unresectable large HCC at the hepatic hilum, Cardiovasc. Intervent. Radiol. 44 (2021) 1462–1466, https://doi.org/10.1007/S00270-021-02841-1.

[27] H. Falk Hansen, M. Bourke, T. Stigaard, J. Clover, M. Buckley, M. O'Riordain, et al., Electrochemotherapy for colorectal cancer using endoscopic electroporation: a phase 1 clinical study, Endosc. Int. Open 8 (2020) E124–E132, https://doi.org/10.1055/A-1027-6735.

[28] F.M. Schipilliti, M. Onorato, G. Arrivi, M. Panebianco, D. Lerinò, A. Milano, et al., Electrochemotherapy for solid tumors: literature review and presentation of a novel endoscopic approach, Radiol. Oncol. 56 (2022) 285–291, https://doi.org/10.2478/RAON-2022-0022.

[29] A.I. Daud, R.C. DeConti, S. Andrews, P. Urbas, A.I. Riker, V.K. Sondak, et al., Phase I trial of interleukin-12 plasmid electroporation in patients with metastatic melanoma, J. Clin. Oncol. 26 (2008) 5896–5903, https://doi.org/10.1200/JCO.2007.15.6794.

[30] Y. Dollin, J. Rubin, R.D. Carvajal, H. Rached, J.R. Nitzkorski, Pembrolizumab and tavokinogene telseplasmid electroporation in metastatic melanoma, Int. J. Surg. Case Rep. 77 (2020) 591–594, https://doi.org/10.1016/J.IJSCR.2020.11.063.

[31] A. Algazi, S. Bhatia, S. Agarwala, M. Molina, K. Lewis, M. Faries, et al., Intratumoral delivery of tavokinogene telseplasmid yields systemic immune responses in metastatic melanoma patients, Ann. Oncol. 31 (2020) 532–540, https://doi.org/10.1016/j.annonc.2019.12.008.

[32] A. Groselj, M. Bosnjak, T. Jesenko, M. Cemazar, B. Markelc, P. Strojan, et al., Treatment of skin tumors with intratumoral interleukin 12 gene electrotransfer in the head and neck region: a first-in-human clinical trial protocol, Radiol Oncol 56 (2022) 398–408, https://doi.org/10.2478/RAON-2022-0021.

[33] P. Strojan, T. Jesenko, M. Omerzel, C. Jamsek, A. Groselj, U.L. Tratar, et al., Phase I trial of phIL12 plasmid intratumoral gene electrotransfer in patients with basal cell carcinoma in head and neck region, Eur. J. Surg. Oncol. (2025) 51, https://doi.org/10.1016/J.EJSO.2025.109574.

[34] B. Dapas, R. Farra, M. Grassi, C. Giansante, N. Fiotti, L. Uxa, et al., Role of E2F1-cyclin E1-cyclin E2 circuit in human coronary smooth muscle cell proliferation and therapeutic potential of its downregulation by siRNAs, Mol. Med. 15 (2009) 297–306, https://doi.org/10.2119/MOLMED.2009.00030.

[35] R. Farra, B. Scaggiante, C. Guerra, G. Pozzato, M. Grassi, F. Zanconati, et al., Dissecting the role of the elongation factor 1A isoforms in hepatocellular carcinoma cells by liposome-mediated delivery of siRNAs, Int. J. Pharm. 525 (2017) 367–376, https://doi.org/10.1016/J.IJPHARM.2017.02.031.

[36] N. Percie du Sert, V. Hurst, A. Ahluwalia, S. Alam, M.T. Avey, M. Baker, et al., The ARRIVE guidelines 2.0: updated guidelines for reporting animal research, Br. J. Pharmacol. 177 (2020) 3617–3624, https://doi.org/10.1111/BPH.15193.

[37] A.J. Smith, R.E. Clutton, E. Lilley, K.E.A. Hansen, T. Brattelid, PREPARE: guidelines for planning animal research and testing, Lab. Anim 52 (2018) 135–141, https://doi.org/10.1177/0023677217724823.

[38] S.I. De Vleeschauwer, M. van de Ven, A. Oudin, K. Debusschere, K. Connor, A. T. Byrne, et al., OBSERVE: guidelines for the refinement of rodent cancer models, Nat. Protoc. 19 (2024) 2571–2596, https://doi.org/10.1038/S41596-024-00998-W.

[39] S. Sachdev, T. Potočnik, L. Rems, D. Miklavčič, Revisiting the role of pulsed electric fields in overcoming the barriers to in vivo gene electrotransfer, Bioelectrochemistry (2022) 144, https://doi.org/10.1016/J.BIOELECHEM.2021.107994.
[40] T. Komel, M. Omerzel, U. Kamensek, K. Znidar, U. Lampreht Tratar, S. Kranjc Brezar, et al., Gene immunotherapy of Colon carcinoma with IL-2 and IL-12 using gene Electrotransfer, Int. J. Mol. Sci. (2023) 24, https://doi.org/10.3390/IJMS241612900.
[41] T. Komel, M. Bosnjak, S. Kranjc Brezar, M. De Robertis, M. Mastrodonato, G. Scillitani, et al., Gene electrotransfer of IL-2 and IL-12 plasmids effectively eradicated murine B16.F10 melanoma, Bioelectrochemistry (2021) 141, https://doi.org/10.1016/J.BIOELECHEM.2021.107843.
[42] M. Cemazar, I. Wilson, G.U. Dachs, G.M. Tozer, G. Sersa, Direct visualization of electroporation-assisted in vivo gene delivery to tumors using intravital microscopy - spatial and time dependent distribution, BMC Cancer (2004) 4, https://doi.org/10.1186/1471-2407-4-81.
[43] Čemažar M, Miklavčič D, Vodovnik L, Jarm T, Rudolf Z, Štabne B, et al. Improved therapeutic effect of electrochemotherapy with cisplatin by intratumoral drug administration and changing of electrode orientation for electropermeabilization on EAT tumor model in mice. Radiology Oncol 1995;29:121–8.
[44] M. Egli, M. Manoharan, Chemistry, structure and function of approved oligonucleotide therapeutics, Nucleic Acids Res. 51 (2023) 2529–2573, https://doi.org/10.1093/NAR/GKAD067.
[45] Y. Han, S.H. Shin, C.G. Lim, Y.H. Heo, I.Y. Choi, H.H. Kim, Synthetic RNA therapeutics in Cancer, J. Pharmacol. Exp. Ther. 386 (2023) 212–223, https://doi.org/10.1124/JPET.123.001587.
[46] T.J. Dweh, G.J.E. Wulu, J.K. Jallah, D.L. Miller, J.P. Sahoo, Innovations in RNA therapeutics: a review of recent advances and emerging technologies, Nucleosides Nucleotides Nucleic Acids (2025), https://doi.org/10.1080/15257770.2025.2451377.
[47] F. Perrone, E.F. Craparo, M. Cemazar, U. Kamensek, S.E. Drago, B. Dapas, et al., Targeted delivery of siRNAs against hepatocellular carcinoma-related genes by a galactosylated polyaspartamide copolymer, J. Control. Release 330 (2021) 1132–1151, https://doi.org/10.1016/J.JCONREL.2020.11.020.
[48] D.G. Johnson, R. Vélez-Cruz, E2F1 and p53 transcription factors as accessory factors for nucleotide excision repair, Int. J. Mol. Sci. 13 (2012) 13554–13568, https://doi.org/10.3390/IJMS131013554.
[49] P.D. Denechaud, L. Fajas, A. Giralt, E2F1, a novel regulator of metabolism, Front. Endocrinol. (Lausanne) (2017) 8, https://doi.org/10.3389/FENDO.2017.00311.
[50] A. Muralidharan, P.E. Boukany, Electrotransfer for nucleic acid and protein delivery, Trends Biotechnol. 42 (2024) 780–798, https://doi.org/10.1016/J.TIBTECH.2023.11.009.
[51] M. Bosnjak, K. Znidar, A. Sales Conniff, T. Jesenko, B. Markelc, N. Semenova, et al., In vitro and in vivo correlation of skin and cellular responses to nucleic acid delivery, Biomed. Pharmacother. (2022) 150, https://doi.org/10.1016/J.BIOPHA.2022.113088.
[52] M. Sioud, Advances in RNA sensing by the immune system: separation of siRNA unwanted effects from RNA interference, Methods Mol. Biol. 629 (2010) 33–52, https://doi.org/10.1007/978-1-60761-657-3_3.
[53] M. Aldea, F. Andre, A. Marabelle, S. Dogan, F. Barlesi, J.C. Soria, Overcoming resistance to tumor-targeted and immune-targeted therapies, Cancer Discov. 11 (2021) 874–899, https://doi.org/10.1158/2159-8290.CD-20-1638.
[54] S. Guo, A. Donate, G. Basu, C. Lundberg, L. Heller, R. Heller, Electro-gene transfer to skin using a noninvasive multielectrode array, J. Control. Release 151 (2011) 256–262, https://doi.org/10.1016/J.JCONREL.2011.01.014.
[55] S. Kos, K. Vanvarenberg, T. Dolinsek, M. Cemazar, J. Jelenc, V. Préat, et al., Gene electrotransfer into skin using noninvasive multi-electrode array for vaccination and wound healing, Bioelectrochemistry 114 (2017) 33–41, https://doi.org/10.1016/J.BIOELECHEM.2016.12.002.
[56] S. Kos, T. Blagus, M. Cemazar, U. Lampreht Tratar, M. Stimac, L. Prosen, et al., Electrotransfer parameters as a tool for controlled and targeted gene expression in skin, Mol. Ther. Nucl. Acids 5 (2016) e356, https://doi.org/10.1038/mtna.2016.65.
[57] N. Semenova, M. Bosnjak, B. Markelc, K. Znidar, M. Cemazar, L. Heller, Multiple cytosolic DNA sensors bind plasmid DNA after transfection, Nucleic Acids Res. 47 (2019) 10235–10246, https://doi.org/10.1093/nar/gkz768.
[58] T. Batista Napotnik, T. Polajžer, D. Miklavčič, Cell death due to electroporation - a review, Bioelectrochemistry (2021) 141, https://doi.org/10.1016/J.BIOELECHEM.2021.107871.
[59] M. Stimac, U. Kamensek, M. Cemazar, S. Kranjc, A. Coer, G. Sersa, Tumor radiosensitization by gene therapy against endoglin, Cancer Gene Ther. 23 (2016) 214–220, https://doi.org/10.1038/CGT.2016.20.
[60] M. Scuderi, J. Dermol-Cern, J. Scancar, S. Markovic, L. Rems, D. Miklavcic, The equivalence of different types of electric pulses for electrochemotherapy with cisplatin - an in vitro study, Radiol. Oncol. 58 (2024) 51–66, https://doi.org/10.2478/RAON-2024-0005.
[61] G. Sersa, K. Ursic, M. Cemazar, R. Heller, M. Bosnjak, L.G. Campana, Biological factors of the tumour response to electrochemotherapy: review of the evidence and a research roadmap, Eur. J. Surg. Oncol. (2021), https://doi.org/10.1016/j.ejso.2021.03.229.